

Investigation of the breakpoint region in stacks with a finite number of intrinsic Josephson junctions

Yu. M. Shukrinov ¹, F. M. ahfouzi ², and N. F. Pedersen ³

¹ BLTP, JINR, Dubna, Moscow Region, 141980, Russia

² Institute for Advanced Studies in Basic Sciences, P.O.Box 45195-1159, Zanjan, Iran

³Oersted-DTU, Section of Electric Power Engineering,

Technical University of Denmark, DK-2800, Lyngby, Denmark

(Dated: March 23, 2024)

We study the breakpoint region on the outermost branch of current-voltage characteristics of the stacks with different number of intrinsic Josephson junctions. We show that at periodic boundary conditions the breakpoint region is absent for stacks with even number of junctions. For stacks with odd number of junctions and for stacks with nonperiodic boundary conditions the breakpoint current is increased with number of junctions and saturated at the value corresponding to the periodic boundary conditions. The region of saturation and the saturated value depend on the coupling between junctions. We explain the results by the parametric resonance at the breakpoint and excitation of the longitudinal plasma wave by Josephson oscillations. A way for the diagnostics of the junctions in the stack is proposed.

I. INTRODUCTION

A series of experiments devoted to intrinsic Josephson junctions¹ (IJJ) shows the growing interest in the current-voltage characteristics (IVC) of the finite stack.^{2,3,4} Different kinds of couplings between intrinsic Josephson junctions determine a variety of the IVC observed in HTSC and different models are exploited for their descriptions. Among them are the inductive⁵ and capacitive coupling^{6,7} models, which usually give approximately similar results. A unified theory for magnetic and electric coupling in multistacked Josephson junctions was developed.⁸ The capacitively coupled Josephson junction model (CCJJ) seizes the main dynamical properties of the IJJ system, describes the multibranch structure in the IVC of the stack of IJJ^{6,9} and explains the microwave resonant absorption.¹⁰ On the other side a diusion current plays an important role in the stack of IJJ¹¹. The CCJJ model with diusion current (CCJJ+DC model) was derived in Ref.12 on the microscopic level. It gives an equidistant branch structure.¹³ Close to the hysteresis jump the system of IJJ is unstable towards a switching. A resonance between the Josephson and plasma oscillations causes the system to switch to another branch. This mechanism in case of one Josephson junction has been considered long time ago.¹⁴

The "breakpoint region" (BPR) on the IVC of the stack of IJJ was demonstrated in Ref.15 and it is explained as a result of resonance between Josephson and plasma oscillations. We consider, that simulation of the IVC of IJJ by different groups using different models shows the BPR on the outermost branch as well, but the authors did not mention it (see particularly, Fig.3a in Ref.7 in CCJJ model; Fig.1 in Ref.11 in charge imbalance (CIB) model; Fig.2 (left) in Ref.16 in CIB model). To our knowledge, no precise experiment to observe the BPR has been carried out yet.

In this paper we show that a detailed investigation of the breakpoint current I_{bp} and BPR width w_{bp} gives

us new important information concerning the creation of longitudinal plasma waves (LPW) in stacks of IJJ and the peculiarities of the stacks with a finite number of IJJ. We study the IVC of IJJ in the framework of the CCJJ+DC model and investigate the dependence of the I_{bp} and the w_{bp} on the number of junctions N in the stack. We demonstrate the existence of the BPR on the branches corresponding to the stack with one oscillating junction (O-junction) and show that such information may allow to develop a new method for the diagnostics of the IJJ.

II. MODEL AND METHOD

In the CCJJ model⁶ a relation between the charge χ_1 and the generalized scalar potential ϕ_1 of the 1-th layer is $\chi_1 = \frac{1}{4\pi r_D^2} \phi_1$, where r_D is Debye screening length and ϕ_1 is expressed through a scalar potential ψ_1 and derivative of phase θ_1 of superconducting condensate by $\dot{\phi}_1(t) = \frac{1}{2e} \frac{\partial \psi_1}{\partial t}$.^{6,11} The last relation reflects a nonequilibrium nature of the ac Josephson effect in layered superconductors¹¹. The superconducting layers are in nonequilibrium state due to the injection of quasiparticles and Cooper pairs. In the equilibrium state $\dot{\phi}_1(t) = 0$. In the CCJJ+DC model¹³ with diusion current $J_D^1 = -\frac{1}{R} \frac{d\chi_1}{dt}$ between layers 1 and 1+1 the total external current through the stack has a form

$$J = C \frac{dV_1}{dt} + J_c^1 \sin(\theta_1) + \frac{1}{2eR} \dot{\phi}_1; \quad (1)$$

where V_1 is the voltage between superconducting layers 1+1 and 1 (see below), θ_1 is the gauge-invariant phase difference $\theta_1(t) = \chi_{1+1}(t) - \chi_1(t) - \frac{2e}{R} \int_1^{1+1} dz A_z(z,t)$ between layers 1+1 and 1, R is junction's resistance, A_z is the vector potential in the barrier. This total external current is different from the current in the CCJJ model by third term in the right hand side of the equation (1).

In the CCJJ model it is equal to $V_1 = R$. As a result, in the CCJJ+DC model we obtain the following system of dynamical equations for the phase differences' ψ_1

$$\theta^2, \quad _1=\theta t^2 = \frac{X}{t^2} \quad A_{110} [I - \sin' t] \quad \theta' t = \theta t] \quad (2)$$

with matrix A

$$A = \begin{matrix} & 0 & 1+G & & 0 & \cdots & & 1 \\ & \begin{matrix} B \\ \vdots \\ C \end{matrix} & 0 & 1+2 & 1+2 & 0 & \cdots & \begin{matrix} C \\ \vdots \\ A \end{matrix} \\ & \begin{matrix} \bar{B} \\ \vdots \\ \bar{C} \end{matrix} & \begin{matrix} \bar{0} \\ \vdots \\ \bar{\cdots} \end{matrix} & & \begin{matrix} \bar{0} \\ \vdots \\ \bar{\cdots} \end{matrix} & & \begin{matrix} \bar{0} \\ \vdots \\ \bar{\cdots} \end{matrix} & (3) \end{matrix}$$

where l^0 runs over all N junctions, parameter gives the coupling between junctions, is dissipation parameter ($\gamma^2 = 1 = c$, where $c = \omega_p^2 R^2 C^2$ is M parameter, ω_p is the plasma frequency and C is the capacity of the junction), I is external current normalized to the critical current I_c , $G = 1 + \dots$, $s = s_0 = s = s_N$ and s, s_0, s_N are the thickness of the middle, first and last S-layers, respectively. In the equation (2) time is normalized to the plasma frequency ω_p .¹⁷ According to the proximity effect we consider that the thickness of the first and last layers are different from the layers inside of the stack. Nonperiodic boundary conditions (BC) are characterized by parameter and the equations for the first and last layers in the system (2) are different from the equation for the middle S-layer.^{6,17} For periodic BC the matrix A has the form

$$A = \begin{matrix} & 0 & 1+2 & & 0 & \cdots & & 1 \\ \begin{matrix} B \\ B \\ B \\ B \\ B \\ \end{matrix} & 0 & & 1+2 & & 0 & \cdots & C \\ & \cdots \\ & & & & & & 0 & A \\ & & & & & & & 1+2 \end{matrix} \quad (4)$$

We solve this system for the stacks with different number N of intrinsic junctions. The numerical procedure has been done as follows. For a given set of model parameters N, \dots , we simulate the IVC of the system, i.e. $V_1(I)$, increasing I from zero up and then down. A change in the parameters N, \dots changes the branch structure in the IVC essentially. Their influence on the IVC in the CCJJ and CCJJ+DC models was discussed in Refs. 9, 13, 17. To calculate the voltages $V_1(I)$ in each point of IVC (for each value of I), we simulate the dynamics of the phases $\varphi_1(t)$ by solving system of equations (2) using fourth order Runge-Kutta method. After simulation of the phase dynamics we calculate the dc voltages on each junction as

$$@'_{10} = @t^X_{10} A_{110} V_{10} \quad (5)$$

where V_1 is normalized to the $V_0 = \sim!_p = (2e)$. The average of voltage V_1 is given by

$$V_1 = \frac{1}{T_{m_{max}} - T_{m_{in}}} \int_{T_{m_{in}}}^{T_{m_{ax}}} V_1 dt \quad (6)$$

where T_m in and T_{max} determine the interval for the averaging. After completing the voltage averaging for current I , the current I is increased or decreased by a small amount ΔI to calculate the voltages in the next point of the IVC. We use a distribution of phases and their derivatives achieved in the previous point of the IVC as an initial distribution for the current point.

Numerical stability was checked by doubling and dividing in half the temporal discretization steps Δt and checking the influence on the IVC. Finally we can obtain the total dc voltage V of the stack by

$$V = \sum_{l=1}^N V_l \quad (7)$$

At some current I some junction (or junctions) switches to the nonzero voltage state and gives some branch of the IVC. We plot the total IVC at different parameters of the problem. The details concerning the numerical procedure are given in Refs.7,17.

To investigate the BPR in detail, we have calculated the IVC for different boundary conditions for the stacks with different number N of IJJ from $N = 3$ to $N = 30$. For clarity we restrict the number of curves in some figures.

III. IVC FOR THE STACKS WITH DIFFERENT NUMBER OF IJJs.

Result of simulation of the total branch structure in the IVC for the stack of 10 IJJ in the C C JJ+ D C model by the equation (2) is presented in the insert of Fig. 1a. As we can see, this IVC demonstrates the BPR on the outermost branch.

The outermost branch corresponds to the state of the stack with all junctions in the rotating state (R-state)¹⁷ and it is the upper branch in the IVC. The values of the breakpoint current I_{bp} and transition current I_j (the jump point to the next branch in the IVC) on the outermost branch are shown by arrows in Fig. 1a. The distance between these two values we call as the width w_{bp} of the BPR. We have found that the breakpoint current I_{bp} and BPR width w_{bp} depend on the parameters and boundary conditions and number of junctions in the stack.

Let us first describe the main features of the BPR which follow from the results of the simulation. As we can see in Fig. 1a, at $\tau = 0$ both I_{bp} and I_j are increased with N , but the increase of the I_{bp} is monotonic. The IVC of the stacks with even N have larger w_{bp} at small N . The IVC in the BPR shows a chaotic behavior and its width is decreased with N . There is a saturation of N -dependence of the I_{bp} at large N .

At $t = 1$ (Fig. 1b) these features remain unchanged but the value of the w_{bp} is decreased for all stacks, especially for $N = 4$ and it is equal to zero for $N = 3$. This

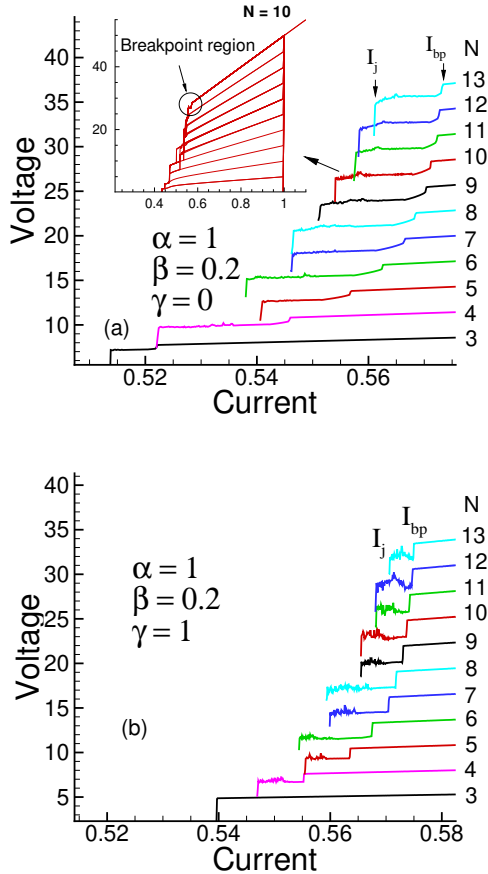


FIG .1: (Color online) (a) – IVC of the outermost branch for the stacks with di erent number N of IJJ at $= 0$; (b) – the same at $= 1$.

change in the boundary conditions leads to the relative changing of the BPR width in di erent stacks as well.

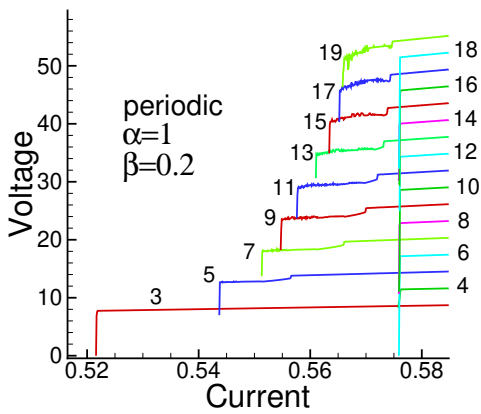


FIG .2: (Color online) IVC of the outermost branch for the stacks with di erent number of junctions at periodic BC .

The IVC at periodic boundary condition (Fig.2) show

the same behavior for the I_{bp} and BPR width w_{bp} for the stacks with odd N as in the nonperiodic case, but for the stacks with even N the value of the I_{bp} does not depend on the N and the BPR for these stacks is absent.

In Fig.3a the I_{bp} as a function of N for $= 0$ (squares, curve 1) and periodic (circles, curve 2) boundary conditions at di erent value of the coupling parameter is presented. We stress the coincidence of the N -dependencies of the I_{bp} for stacks with odd numbers of IJJ for periodic and $= 0$ cases. The increase in α leads to the saturation of the N -dependence at larger N . The value of saturated I_{bp} is decreased with coupling and consists of 0.576 at $\alpha = 1$, 0.454 at $\alpha = 0.5$ and 0.304 at $\alpha = 0.1$. At $\alpha = 0$ the breakpoint coincides with the return current, so the I_{bp} has the same value for the stacks with di erent number of junctions.

The N -dependence of the BPR width w_{bp} for stacks with even and odd number of junctions at $= 0$ (curves 1_{even} and 1_{odd}) and periodic (curve 2_{odd}) boundary conditions is shown in Fig.3b. The main feature here is a decrease of the BPR width w_{bp} with N at large N . At small N in the interval (3,6) we observe the increase of the w_{bp} with N .

IV . THE ORIGIN OF THE BREAKPOINT ON THE OUTERMOST BRANCH

To explain the observed features of the nite stacks IVC let us discuss the origin of the breakpoint on the outermost branch. The hysteresis jump in the IVC is associated with the change of the distribution pattern of rotating phase motions.¹⁷ But the question "why does a change in the current leads to the change in a distribution pattern of the rotating phase motions" is still open. We consider a case that all junctions are in the rotating state, ie. the time average of ' ψ_1 ' $\langle \psi_1 \rangle = \frac{1}{T_{max}} \int_{T_{min}}^{T_{max}} \psi_1 dt$ is constant and that of $\sin \psi_1$ is zero for these junctions. For the oscillating junctions the situation is opposite: the time average of ' ψ_1 ' is zero and that of $\sin \psi_1$ is constant.

As we mentioned above, the outermost branch in the IVC corresponds to the state of the stack with all junctions in the rotating state. Let us write an equation for the di erence of phase di erences $\psi_1 = \psi_{l+1} - \psi_1$ for the outermost branch.

By subtracting equation (2) for $(l+1)$ th and (l) th junctions we get

$$\langle \psi_{l+1} - \psi_1 \rangle + (1 - r^{(2)}) f_l \sin(\psi_{l+1}) - \sin(\psi_1) + \langle \psi_{l+1} - \psi_1 \rangle g = 0 \quad (8)$$

Here $r^{(2)} f_l = f_{l+1} + f_{l-1} - 2f_l$ is the discrete Laplacian. Consider a linear approximation $\sin(\psi_{l+1}) - \sin(\psi_1) \approx \psi_{l+1} - \psi_1$, where $\psi = \frac{1}{N} V t$, V is Josephson frequency, V is total voltage of the stack, we obtain

$$\psi_{l+1} + (1 - r^{(2)}) (\cos(\psi_{l+1}) - 1) = 0 \quad (9)$$

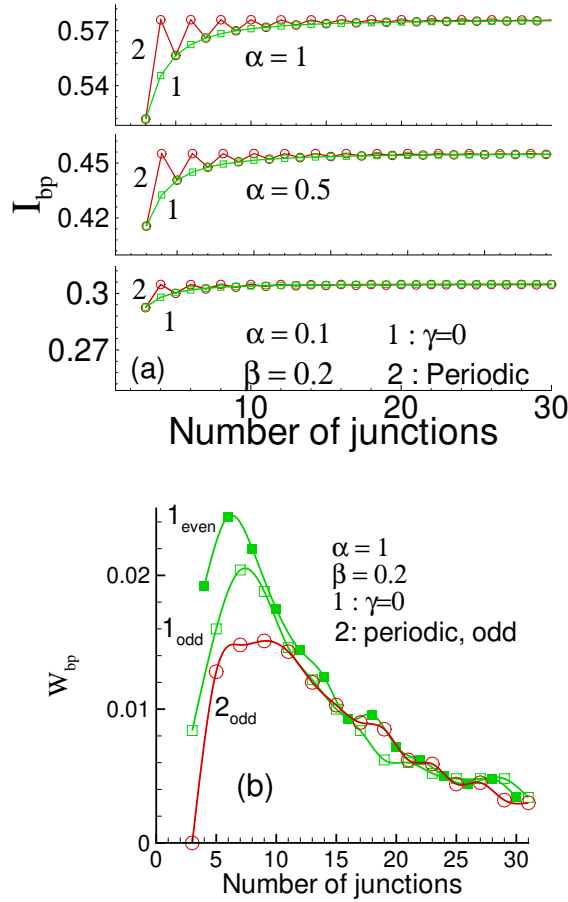


FIG . 3: (Color online) (a) – the N -dependence of the I_{bp} for $\gamma = 0$ (curve 1) and periodic (curve 2) boundary conditions at different α ; (b) – the N -dependence of the BPR width w_{bp} for stacks with even and odd number of junctions at $\gamma = 0$ (1) and periodic (2) boundary conditions.

Expanding $I_1(t)$ in the Fourier series

$$I_1(t) = \sum_k e^{ikt} \quad (10)$$

the linearized equation for the Fourier component of a difference of the phase differences k between neighbor junctions can be written in the form¹⁵

$$k + \langle k \rangle \pi + \cos(\langle k \rangle) k = 0; \quad (11)$$

where $\langle k \rangle = I_p(k) t_p / I_p(k) = I_p C$, $\langle k \rangle = C$, $\langle k \rangle = -C$ and $C = 1/(1 + 2(1 - \cos(k)))$.

The important fact for us is that this linearized equation manifests a parametric resonance in the system of IJJ. In Fig. 4a we plot the resonance region for this equation on the diagram (k) – (k) . The dark stripe on this figure is actually the distribution of the dots, corresponding to the positions of the breakpoints of the outermost branch. Using the breakpoint values of the voltage in the equation $\langle k \rangle = -C = V/N C$ we obtain this distribution of the breakpoints by the variation of the coupling

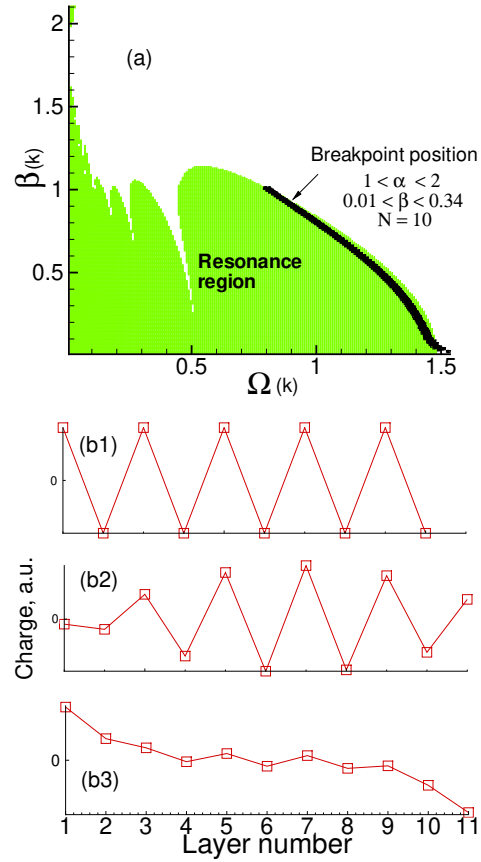


FIG . 4: (Color online) (a) – Parametric resonance region in (k) – (k) diagram. Black dots (stripe) correspond to the breakpoint current I_{bp} in the IV C for $k =$ at different values of parameters α and β ; (b) – Charge on the S-layers in the stacks with 10 IJJ (b1) and 11 IJJ (b2) at periodic BC and with 10 IJJ at $\alpha = 1$ (b3).

parameter in the interval $(1,2)$ with a step 0.1 and the dissipation parameter in the interval $(0.01,0.34)$ with the step 0.01 at each value of β . In contrast to the results presented in Ref.15 where the positions of the dots on the diagram (k) – (k) were obtained by crude estimation, here we have done the precise numerical calculations. This calculations show more close positions of the breakpoints to the boundary of the resonance region in the chosen intervals of α and β . The reason, that the position of the breakpoints are shifted from the boundary of the resonance region in Fig. 4a, is the linear approximation used to obtain the equation (9).

The breakpoints are inside of the resonance region, i.e. the resonance between the Josephson and plasma oscillations is approached at the breakpoint I_{bp} . As a result the plasma mode is excited by the Josephson oscillations. We can prove this statement directly. By Maxwell equation, $\text{div } \mathbf{E} = 4\pi\rho$, we express the charge q_1 on the S-layer 1 by the voltages $V_{1,l+1}$ and $V_{1,l+1}$ in the neighbor insulating layers $q_1 = \frac{1}{4\pi\epsilon_0 d} (V_{1,l+1} - V_{1,l+1})$. The time de-

pendence of the I_{bp} , presented in Fig. 4b1, demonstrates that at periodic BC in the stacks with 10 IJJ the LPW with $k = \pi$ is realized. Really, the charge on the nearest neighbor layers has the same value and an opposite sign. Fig. 4b2 shows the distribution of the charge on the S-layers in the stacks with 11 IJJ at periodic BC. In this case we observe the creation of the LPW with $k = \pi/2$. To determine the mode of the LPW at nonperiodic BC need more detail investigation. Fig. 4b3 demonstrates the charge distribution in the stack with 10 IJJ at $\alpha = 1$ near the breakpoint.

The wavelengths of the standing LPW which can be realized in the stack with N junctions are $N=n$ units of lattice in z-direction, where n changes from 1 to $N=2$ for stacks with even number of junctions and from 1 to $(N-1)/2$ for odd N . The voltage of the stack at the breakpoint is related to the wave number k of the LPW by formulae $V = N(k) = 1 + 2(1 - \cos(k))$, so the largest breakpoint voltage V in the current decreasing process corresponds to the creation of the LPW with k equal to $\pi/2$ (m mode) for stacks with even number of IJJ and modes with $k = (N-1)\pi/N$ for stacks with odd N .

V. DISCUSSION OF THE MAIN RESULTS

Let us now return to the results presented in Fig. 1–Fig. 3 and demonstrate that they are in agreement with the ideas stated in the previous section.

According to these ideas, in the stack with 10 IJJ the LPW with $k = (\pi-1)\pi/10 = \pi/5$ is created and it leads to the increase of the I_{bp} with N and its saturation to the value, corresponding to the m mode. The same modes are created in the stacks with $\alpha = 1$ which outermost branches of the IVC are presented in Fig. 1b. They demonstrate the saturation of the I_{bp} to the same value.

As Fig. 2 shows, at periodic BC we observe the same value of I_{bp} in the all stacks with even N . It is in agreement with our suggestion that in this case the LPW with $k = \pi/2$ is created. We check it directly as well, by the time dependence of the I_{bp} . We find that at periodic BC in the stacks with even N the charge on the nearest neighbor layers has the same value and an opposite sign which means that the LPW with $k = \pi/2$ is realized.

In the stacks with odd N the m mode cannot exist, so as we mentioned in the previous section, the LPW with the largest k equal to $k = (\pi-1)\pi/(N-1) = \pi/4$ is created. The creation of different modes of the LPW leads to the different I_{bp} and this fact explains the difference in the IVC at periodic BC of the stacks with even and odd numbers of IJJ. With increase in N the wave number k limits to $\pi/2$ and it leads to the increase in I_{bp} which we observe in Fig. 2.

It explains as well the saturation of the I_{bp} to the value corresponding to the I_{bp} for stacks with even N which is demonstrated in Fig. 3a.

The difference between the charge distribution on the S-layers at the breakpoint current at fixed time for stacks

with even and odd numbers of IJJ (10 and 11) at periodic BC is demonstrated in Fig. 4b. In the stack with odd N the charge on the first and last layers oscillates in-phase and the oscillations on the neighbor S-layers are different from the oscillations in m mode. Because at $\alpha = 0$ the charge on the first and last layers is screened due to the proximity effect, the LPW with the $k = (\pi-1)\pi/(N-1)$ is also created both for stacks with odd and even N . This is a reason the values of I_{bp} for stacks with odd N coincide for both these BC as shown in Fig. 3a.

At $\alpha = 1$ the same modes are created, but the character of the charge distribution among the S-layers is different (as we can see in Fig. 4b3). As a result in this case the N -dependence of the I_{bp} is stronger than at $\alpha = 0$, but at $N > 1$ it is saturated as well and the saturation value is the I_{bp} for even junctions at periodic BC.

The influence of the coupling parameter on the value of the breakpoint current I_{bp} and its N -dependence which is demonstrated in Fig. 3a has a clear explanation. It consists in the mentioned in the previous section the dependence of the voltage, and correspondingly, the breakpoint current I_{bp} . They are proportional to the term $\frac{1}{1+2(1-\cos(k))}$. An increase in k leads to the term proportional to the $\frac{1}{1+4}$. The decrease in m makes this influence weaker.

We may explain an increase in w_{bp} at small N , which is shown in Fig. 3b by a commensurability effect on the width of the BPR. At periodic BC $w_{bp} = 0$, if the wavelength of the LPW is $\lambda = n$, where $n = 2; 3; 4; \dots$ lattice units in z-direction. As we can see in Fig. 2, at $\alpha = 3$ (for stacks with $N = 3$) and $\alpha = 2$ (m mode), the IVC do not show the BPR. The creation of the LPW with wavelength in the middle of the interval (2,3) should correspond to some maximum of the BPR width w_{bp} . In the stack with 5 IJJ the LPW with $\lambda = 2.5$ ($k = 4\pi/5$) is created. It does not coincide exactly with the result obtained by the simulation, because we use for the explanation the linearized equation for difference of phase differences and Fourier expansion in the finite stacks. The wave number k is not well defined in this case. With increase in N the wave number k of LPW limits to $\pi/2$ and it explains the increase in I_{bp} and the decrease in w_{bp} at large N which demonstrated by Fig. 3b. The change in the boundary conditions changes the character of the charge oscillations on the S-layers. Particularly, at $\alpha = 1$ we observe a decrease in the w_{bp} for all stacks. Our analysis shows that in stacks with even N at nonperiodic BC the charge on the second and $N-1$ layers oscillate in-phase, but anti-phase in the stacks with odd N . We consider that the value of the BPR width w_{bp} depends on the character of the charge oscillations on the S-layers.

Finally, we note that in the case of coupling between junctions the parameter α cannot be determined in a usual way by the return current, because it depends now on two parameters, α and β . The dependence of the I_{bp} and BPR width w_{bp} on the dissipation and coupling parameters opens an opportunity to develop the new

method for determination of these parameters for the stacks of IJJ. This question will be discussed in detail somewhere else.

V I. ONE OSCILLATING JUNCTION

Let us now discuss briefly the breakpoints on the other branches of the IVC.

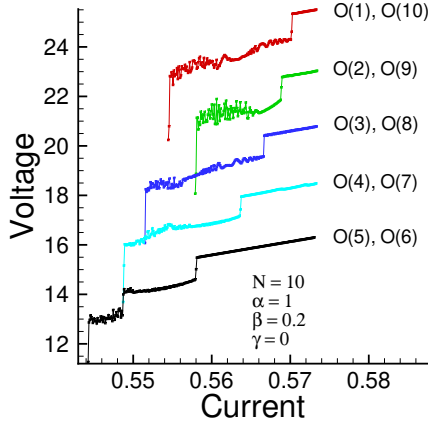


FIG. 5: (Color online) The BPR on the branches of the IVC of the stacks with one oscillating junction in the case of 10 IJJ at $\alpha = 1$, $\beta = 0.2$ and $\gamma = 0$. The upper curve corresponds to the real scale of voltage, but the other ones are shifted for clarity by two units down.

As we mentioned above a resistive state in the system of IJJ is realized as a state with different number of R-and O-junctions.^{9,17} The different positions of R-and O-junctions in the stack (different configurations) correspond to the different states of IJJ system. The equidistant positions of the O-junction from the ends of the stack (for example, the stacks with 1st or 10th O-junction) lead to the same state. So, there are five different states in the stack with one O-junction corresponding to the different position of this junction. Fig. 5 shows the BPR on the branches of the IVC of the stacks with one O-junction in the case of 10 IJJ at $\alpha = 1$, $\beta = 0.2$ and $\gamma = 0$.

The equidistant positions of the O-junction from the ends of the stack lead to the same value of I_{bp} and the same width of BPR. The shift of the O-junction from the end of the stack to its center decreases the I_{bp} of the corresponding state. So, we may establish a delay of the LPW creation in the current decreasing process when the position of the O-junction is shifted to the center of the stack.

We consider that the origin of such behaviour is the next. This one oscillating junction separates the stack in two parts with different number of R-junctions which are weakly coupled through it. With a decrease in cur-

rent the first LPW is created in the part with the largest I_{bp} (with the largest number of junctions). The shift of the O-junction and the decrease in the number of R-junctions in this part lead to the decrease of the I_{bp} as Fig. 1 demonstrates. The increase of the number of junctions in the second part might manifest the second breakpoint which is related to the creation of LPW in this second part of the stack. Such situation is observed for $N = 10$ when O-junction occupies the 5th or 6th site in the stack. The width of the BPR in the other branches of IVC depends essentially on the state of the stack.

For the other branches the increase in the number of the O-junctions in the stack decreases the number of effective junctions for creation of the LPW and it leads to the decrease of the return current. This fact explains why we can obtain a total branch structure in the hysteresis region, because in the other case we would not be able to observe it in the simulation. The correspondence between the position of the O-junction in the stack and the value of the I_{bp} opens the possibility for junction diagnostics, i.e. by measuring the value of the I_{bp} we can answer the question which junction in the stack goes into R-or O-state. From the other side, the monitoring of the transitions between branches is useful for understanding the phase dynamics in the system of IJJ.

V II. CONCLUSIONS

In conclusion, we stress that the BPR in the IVC "naturally" follows from the solution of the system of the dynamical equations for the phase difference for the stack of IJJ. In breakpoint region the plasma mode is a stationary solution of the system and this fact might be used in some applications, particularly, in high frequency devices such as THz oscillators and mixers. The detailed study of the breakpoint current and breakpoint region width gives a new opportunity for the investigation of the properties of IJJ and develop new methods for the determination of the parameters of IJJ and diagnostic of IJJ in the stacks.

V III. ACKNOWLEDGMENTS

We thank P. Muller, R. Kleiner, A. Ustinov, T. Koyama, M. Machida, A. Yurgens, Yu. Latyshev, A. Irie, M. Sargolzaei, T. Boyadzhiev, N. M. Palkida, Y. Sobouti, M. R. H. Kashhpour for stimulating discussions and support of this work.

References

-
- ¹ R .K leiner, F .Stein m eyer, G .K unkeland P .M uller, Phys. Rev.Lett. 68, 2394 (1992); G .O ya, N .A oyama, A .Irie, S .K ishida, and H .Tokutaka, Jpn.J.Appl.Phys., 31, L829 (1992).
- ² M yung-H o Bae, Jae-Hyun Choi, Hu-Jong Lee, cond-m at/0610334.
- ³ L .X .You, M .Torstensson, A .Yurgens, D .W inkler, C .T .Lin, and B .Liang, Appl.Phys.Lett. 88, 222501 (2006).
- ⁴ Y .-J.D oh, H .-J.Lee, and H .-S.Chang, Phys.Rev.B 61, 3620 (2000).Ch.P reis, Ch.H elm , K .Schmalzl, J.K eller, R .K leiner, and P .M uller, Physica C 362,51 (2001).
- ⁵ S.Sakai, P .Bodin, N .F .Pedersen, J.Appl.Phys.73, 2411 (1993).
- ⁶ T .K oyama and M .Tachiki, Phys.Rev.B 54, 16183 (1996).
- ⁷ M .M achida, T .K oyama, and M .Tachiki, Phys.Rev.Lett. 83, 4618 (1999).
- ⁸ M .M achida, S .Sakai, Phys.Rev.B 70, 144520 (2004).
- ⁹ Yu.M .Shukrinov and F .M ahfouzi, Physica C 434, 6 (2006).
- ¹⁰ Y .M atsuda, M .B .G aifullin, K .K umagai, K .K adowaki, T .M ochiku, Phys.Rev.Lett. 75, 4512 (1995).
- ¹¹ D .A .Ryndyk, Phys.Rev.Lett. 80, 3376 (1998).
- ¹² M .M achida, T .K oyama, A .Tanaka and M .Tachiki, Physica C 330, 85 (2000).
- ¹³ Yu.M .Shukrinov, F .M ahfouzi, P .Seidel, Physica C 449, 62 (2006).
- ¹⁴ N .F .Pedersen, J.M ygind, O .H .Soerensen, and B .D ueholm , J.de Phys.C 6, 1232 (1978); H .H .Zappe, J.Appl.Phys. 44, 1371 (1973).
- ¹⁵ Yu.M .Shukrinov, F .M ahfouzi, Supercond.Sci.Technol., 20, S38, (2007).
- ¹⁶ Yu.M .Shukrinov and F .M ahfouzi, J.Phys.Conf.Ser.43, 1143 (2006).
- ¹⁷ H .M atsumoto, S .Sakamoto, F .W ajima, T .K oyama, M .M achida, Phys.Rev.B 60, 3666 (1999).